Voltage dependence of macroscopic and unitary currents of gap junction channels formed by mouse connexin50 expressed in rat neuroblastoma cells

Miduturu Srinivas*, Mauro Costa†, Yang Gao*, Alfredo Fort*, Glenn I. Fishman‡ and David C. Spray*†

*Department of Neuroscience, Albert Einstein College of Medicine, Bronx, NY 10461, USA, †Laboratory of Excitable Membranes, Instituto de Biofisica Carlos Chagas Filho, Federal University of Rio de Janeiro, Rio de Janeiro, Brazil and ‡Cardiovascular Institute, Section of Myocardial Biology, Mount Sinai School of Medicine, NY 10029, USA

(Received 25 November 1998; accepted after revision 3 March 1999)

1. The macroscopic and single channel gating characteristics of connexin (Cx) 50 gap junction channels between pairs of N2A neuroblastoma cells transfected with mouse Cx50 DNA were investigated using the dual whole-cell voltage clamp technique.

2. The macroscopic junctional current (I_j) of Cx50-transfected cells decayed exponentially with time in response to transjunctional voltage (V_j) steps (time constant (τ) of ~4 s at a V_j of 30–40 mV and 100–200 ms at a V_j of 80–100 mV). The steady-state junctional conductance (g_j) was well described by a two-state Boltzmann equation. The half-inactivation voltage (V_0), the ratio of minimal to maximal g_j (g_{min}/g_{max}) and the equivalent gating charge were ±37 mV, 0·21 and 4, respectively.

3. The conductance of single Cx50 channels measured using patch pipettes containing 130 mM CsCl was 220 ± 13·1 pS (12 cell pairs). A prominent residual or subconductance state corresponding to 43 ± 4·2 pS (10 cell pairs) was also observed at large V_js.

4. The relationship between channel open probability (P_o) and V_j was well described by a Boltzmann relationship with parameters similar to those obtained for macroscopic g_j ($V_0 = 34$ mV, gating charge = 4·25, maximum $P_o = 0·98$). The ensemble average of single channel currents at $V_j = 50$ mV declined in a monoexponential manner ($\tau = 905$ ms), a value similar to the decline of the macroscopic I_j of Cx50 channels at the same voltage.

5. Ion substitution experiments indicated that Cx50 channels have a lower permeability to anions than to cations (transjunctional conductance of KCl *vs.* potassium glutamate ($\gamma_{j,KCl}/\gamma_{j,KGlut}$), 1·2; 6 cell pairs).

6. The results have important implications for understanding the role of connexins in tissues where Cx50 is a major gap junction component, including the lens.

Gap junction channels provide pathways of intercellular communication, allowing the passage of ions and small molecules up to 1 kDa in mass or up to 14 nm in diameter (Simpson *et al.* 1977). A single gap junction channel is formed by the association of two hemichannels which are located in the plasma membranes of adjacent cells. Each hemichannel (or connexon) is a hexameric complex of a family of protein molecules known as connexins (Bennett *et al.* 1991; Yeager & Gilula, 1992; Bruzzone *et al.* 1996). At least 14 different connexin (Cx) subtypes have been identified thus far in rodents; connexin proteins are named according to species of origin and molecular weight (e.g. mouse connexin50). Each connexin subtype forms gap junction channels that have unique biophysical properties such as sensitivity to gating by transjunctional voltage (i.e. the difference in voltage between the cytoplasms of two adjacent cells) (e.g. Spray *et al.* 1979; Moreno *et al.* 1991*b*; Barrio *et al.* 1991), by phosphorylation (Moreno *et al.* 1994*b*; Kwak *et al.* 1995) and by cytoplasmic acidification (Morley *et al.* 1997; Lin *et al.* 1998). Moreover, gap junctions formed by the various connexins have distinct single channel conductances (e.g. Moreno *et al.* 1991*b*; Reed *et al.* 1993; Bukauskas *et al.* 1995) and unique anion : cation permeability ratios (Veenstra *et al.* 1995).

Genomic DNA encoding Cx50 was cloned and sequenced in a collaborative effort between the laboratories of Drs Jorge Kistler, Daniel A. Goodenough and David L. Paul and was shown to be identical to the MP70 protein that is highly

expressed between lens fibre cells (Kistler *et al.* 1985; White *et al.* 1992). It is now known that the rodent lens expresses three different connexins: Cx43 is found between epithelial cells whereas Cx46 and Cx50 are expressed between lens fibre cells (Paul *et al.* 1991; Yancey *et al.* 1992; White *et al.* 1992; for reviews see Goodenough, 1992; Mathias *et al.* 1997). In addition, Cx50 has been reported to be expressed in corneal epithelial cells (Wolosin *et al.* 1997), macroglial cells of the optic nerve (Schutte *et al.* 1998) and in cardiac valve tissue (Gourdie *et al.* 1992).

Connexin-mediated intercellular communication in lens has been proposed to be necessary for the maintenance of precise intracellular ionic concentrations in the encysted fibre cells and for prevention of cataract formation (Goodenough, 1992; Mathias *et al.* 1997). Direct confirmation of such a role has been provided by transgenic mice lacking expression of lens connexins, and by linkage studies of certain cataractous human diseases. Transgenic mice lacking Cx50 or Cx46 develop nuclear cataracts (Gong *et al.* 1997; White *et al.* 1998), whereas lenses of neonatal Cx43 knockout mice display anatomical abnormalities similar to those detected in early stages of osmotic cataract (Gao & Spray, 1998). In addition, the lenses of Cx50 knockout mice are smaller than normal, implying an early developmental defect (White *et al.* 1998). Genetic linkage analysis has suggested that Cx46 and Cx50 may be the culprit genes in rare familial cataractous conditions (Steele *et al.* 1997; Mackay *et al.* 1997; Shiels *et al.* 1998), and in the case of Cx50, the defects have been traced to point mutations in the first extracellular domain (Steele *et al.* 1997) and in the second transmembrane domain (Shiels *et al.* 1998). The lack of complete rescue of lens function in animal models and human diseases in which one connexin is functionally ablated strongly indicates that each of these connexins provides a unique complement in maintaining normal lens function. Thus, a detailed knowledge of the functional properties of the lens connexins would be useful in assessing their relative contributions to both normal and pathological lens functions.

The biophysical properties of Cx43 gap junction channels have been well characterized in cells dissociated from a variety of Cx43-expressing tissues and following exogenous expression in *Xenopus* oocytes and mammalian cells (White *et al.* 1994; Moreno *et al.* 1995). In contrast, little is known regarding the properties of junctional channels formed by Cx50 or Cx46. Electrophysiological studies on oocyte pairs that had been injected with Cx50 cRNA revealed that gap junction channels formed by Cx50 are strongly sensitive to transjunctional voltage (White *et al.* 1994). However, the low input resistance of *Xenopus* oocytes precluded measurement of single channel properties of Cx50 gap junctions. Application of the dual whole-cell patch clamp technique to differentiating fibre cell pairs indicated that the gap junction channels of these cells are strongly voltage dependent and exhibit single channel junctional currents corresponding to a range of unitary conductance values (Donaldson *et al.* 1995). Because of the existence of both Cx46 and Cx50, as well as trace amounts of Cx43, in these cells, however, it was not possible to attribute these conductance values to channels formed of any single connexin.

In order to define the characteristics of Cx50 gap junction channels, we have investigated their properties in a communication-deficient mammalian cell line following stable transfection with Cx50 cDNA, a strategy that has been successful for other connexins since its introduction almost a decade ago (Eghbali *et al.* 1990). Findings from these experiments demonstrate that Cx50 forms large conductance gap junction channels in mammalian cells that are strongly sensitive to transjunctional voltage, and are more permeant to cations than to anions.

METHODS

DNA construction and transfection

A fragment of genomic Cx50 corresponding to the full length coding region (generously provided by Dr David L. Paul, Harvard Medical School, Boston, MA, USA) was subcloned into the expression vector pCDNA3 (Invitrogen, Carlsbad, CA, USA) at the *Bam*H1–*Eco*RV restriction site. N2A rat neuroblastoma cells (obtained from ATCC, Rockville, MD, USA, and subcloned by dilution to generate a parental cell line that expressed only minimal endogenous Cx45) were transfected with 6 μg of DNA using the LIPOfectamine reagent (Gibco BRL, Gaithersberg, MD, USA). After 48 h, the cells were transferred to selection medium containing 0·5 μg ml^{-1} G418 (Gibco BRL). Individual clones were picked after 2 weeks, grown to confluence over a period of an additional 1–3 weeks, and then tested for expression of Cx50 mRNA by Northern blot analysis. Cells were passaged and maintained continuously in G418-containing media; early passages of cells were frozen at each splitting of confluent cultures. All cell cultures were maintained in a 37 °C incubator in a moist 5% CO_2–95% air environment.

Northern blot analysis of transfected N2A cells

Total RNA was prepared from each individual clone grown in 60 mm dishes using TRIzol (BRL, Grand Island, NY, USA). Equal amounts of RNA were electrophoresed on 1% agarose–formaldehyde gels and transferred onto nitrocellulose membranes using 20× saline–sodium citrate (SSC) buffer (3 M NaCl, 0·3 M sodium citrate, pH 7·5) for 12 h and fixed by exposure to UV light (Stratalink, Stratagene, La Jolla, CA, USA). ^{32}P probes were generated using the entire coding region by random priming (Prime-It; Stratagene) in the presence of 50 μCi of ^{32}P-dCTP (NEN, Boston, MA, USA). The membranes were then prehybridized for 30 min at 68 °C using QuickHyb solution (Stratagene) and hybridized for 1 h at 68 °C. Filters were washed twice with 2× SSC–0·1% SDS at room temperature, once in 0·1× SSC–0·1% SDS at 60 °C and exposed to X-ray film.

Immunocytochemistry

Indirect immunofluorescence labelling of Cx50 in N2A transfected cells and in mouse eye tissues (positive control) was carried out with slight modification of a procedure described previously (Dermeitzel *et al.* 1991). Newborn animals were killed by decapitation; protocols complied with national guidelines and were approved by the Albert Einstein College of Medicine Animal Institute. In brief, cultured cells and cryostat sections (8 μm thick) of the eyeballs of wild-type littermates were fixed on glass coverslips with 3·7% formaldehyde for 10 min and permeabilized in 50% cold acetone for 2 min, 100% acetone for 5 min and 50% acetone for 2 min,

washed with Dulbecco's phosphate buffered saline (PBS, Gibco) and incubated in PBS supplemented with 0·5% bovine serum albumin (essentially globulin free, Sigma, St Louis, MO, USA) in order to block non-specific labelling. The primary antibodies used were anti-Cx50 mouse monoclonal IgG at 1 : 100 dilution in PBS (generously provided by Dr David L. Paul, Harvard Medical School, Boston, MA, USA). The cells and sections were incubated with connexin antibody with pre-immune antiserum overnight at 4 °C. After extensive washing with PBS, coverslips were transferred to new culture dishes and exposed to Alexa 488- conjugated goat anti-rabbit IgG (Molecular Probes) at 1 : 200 dilution at room temperature in the dark for 1 h. Coverslips were washed 5 times with PBS, then briefly with distilled water, and mounted on slides with 0·1% paraphenylenediamine in a 10 : 1 mixture of 33% glycerol and PBS. The cells and specimens on the coverslips were viewed with a Nikon microscope equipped with fluorescein isothiocyanate (FITC) excitation, emission filters and a mercury arc lamp. Non-specific background staining was evaluated in adjacent eyeball sections and clonal N2A cells in which primary antibody was omitted.

Electrophysiology

N2A cells transfected with Cx50 were plated at low density onto 1 cm diameter glass coverslips. Coverslips were transferred to the stage of a Nikon Diaphot microscope and bathed in a external solution containing (mM): NaCl, 140; CsCl, 2; $CaCl_2$, 2; $MgCl_2$, 1; Hepes, 5; KCl, 4; dextrose, 5; pyruvate, 2; $BaCl_2$, 1; pH 7·2. Junctional conductance was measured between cell pairs using the dual whole-cell voltage clamp technique with Axopatch 1C or 1D patch clamp amplifiers (Axon Instruments, Foster City, CA, USA). Each cell of a cell pair was voltage clamped with patch pipettes pulled on a Flaming–Brown Micropipette puller (model P-87, Sutter Instrument Co.). The patch electrodes had resistances of 4–7 MΩ when filled with internal solution containing (mM): CsCl, 130; EGTA, 10; $CaCl_2$, 0·5; MgATP, 3; Na_2ATP, 2; Hepes, 10; pH 7·2. In experiments involving ionic substitutions, CsCl was replaced by equimolar amounts of KCl or potassium glutamate. All experiments were performed at room temperature. The osmolarity of the external and internal solutions measured using the freezing point method (Microosmette, Precision Instruments, Natick, MA, USA) was 285 mosmol l^{-1}. Macroscopic and single channel recordings were filtered at 0·2–1 kHz and sampled at 2–5 kHz, as described in the figure legends. Data acquisition and analysis were performed with pCLAMP6 software (Axon Instruments). Membrane currents were also recorded simultaneously on a strip chart recorder (Gould Brush 2400, Saddle Brook, NJ, USA).

Each cell of a pair was initially held at a common holding potential of 0 mV. Thereafter, voltage pulses of variable duration and amplitude were applied to one cell to establish a transjunctional voltage gradient (V_j) and the junctional current was measured in the second cell (held at 0 mV). Macroscopic junctional conductance (g_j) was calculated by dividing the measured junctional current by the transjunctional voltage step. To evaluate the voltage dependence of the junctional conductance, 7–10 s hyperpolarizing or depolarizing pulses were applied every 30 s from the holding potential of 0 mV to various test potentials (between −100 and 100 mV). Only those cell pairs where g_j was between 2 and 4 nS were used to measure macroscopic voltage sensitivity, thereby minimizing the impact of series resistance on these measurements (Moreno *et al.* 1991*b*; Wilders & Jongsma, 1992). The instantaneous and steady-state levels of junctional currents were measured at the beginning and at the end of each V_j pulse. Steady-state junctional current at each voltage was normalized relative to the instantaneous current and these $G_{j,ss}$ values were plotted as a function of the transjunctional voltage. The relationship between $G_{j,ss}$ and V_j was fitted assuming a two-state Boltzmann equation:

$$G_{j,ss} = \{(G_{max} - G_{min})/(1 + \exp[A(V_j - V_0)]\} + G_{min}, \quad (1)$$

where V_0 is the voltage at which the conductance is half-maximal, G_{max} is the maximum normalized conductance, G_{min} is the normalized voltage-insensitive residual conductance and A is a parameter defining the steepness of voltage sensitivity ($A = nqF$, where n is the equivalent number of gating charges of valence q and F is the Faraday constant).

Unitary current events were recognized as simultaneously occurring equal-sized events of opposite polarity in each cell's current recording; these events were measured from freshly split cell pairs and in individual clones where the incidence of coupling was low. Single channel events at different V_j values were recorded for variable duration (usually 1–5 min) as described in the figure legends. All points amplitude histograms of data were constructed for each experiment and data were fitted to Gaussian functions to determine the mean and variance of the baseline and open channel current.

Unitary conductances were measured by fitting a linear function to the single channel current–voltage relationship. Recordings from only those cell pairs that contained one or two channels were used to determine the unitary current amplitudes. Channel open probability (P_o) was determined from both single and multichannel recordings. In cases where cell pairs exhibited a single active Cx50 channel, open probability was estimated as the absolute fraction of time that was spent in the main state. To ensure that stationary conditions were met, we waited at least three time constants (τ) before analysing data for open probability measurements. Open probability was also estimated from multichannel recordings as previously described (Manivannan *et al.* 1992). Briefly, the occupation probabilities at each level (P_r) were determined from the area under each peak from the fit of the normalized amplitude histogram to the Gaussian function. For channels that gate independently, P_r follows a binomial distribution of the form:

$$P_r = \frac{N!}{r!(N-r)!} P_o^{\,r} (1 - P_o)^{N-r}, \quad (2)$$

where $r = 0, 1, 2, \ldots, N$. Fits of P_r values to the binomial equation yielded the channel open probability (P_o) and the number of channels (N). When accurate fits were not obtained under these conditions, the P_r values were fitted to alternative expressions that have been derived for cases where (1) the channels are independent, but not identical and (2) channels are not independent (i.e. display co-operative openings or closings) (Manivannan *et al.* 1992).

Dye coupling

Lucifer Yellow CH (5% w/v in 150 mM LiCl) was injected through a microelectrode (~20 MΩ if filled with 3 M KCl) into one cell of a cluster of N2A Cx50-transfectants using short hyperpolarizing current pulses (Model M4A patch clamp amplifier; Warner Instruments Inc., Hamden, CT, USA). In separate experiments, spread of Lucifer Yellow in pairs of cells was determined in conjunction with the dual whole-cell voltage clamp technique. In these experiments, one patch electrode was filled with the CsCl internal solution containing 20 mM Lucifer Yellow CH and junctional conductance was determined as described above. Dye transfer in clusters or in cell pairs was visualized using a Nikon Diaphot inverted microscope equipped with xenon epifluoroscence illumination and an FITC filter set. Phase contrast and fluorescence micrographs were recorded 1–2 min after dye injection by exposing Kodak TMAX 400 film.

RESULTS

Expression levels, transcript size and strength of functional coupling in Cx50 transfectants

In order to study the functional properties of connexin50 in mammalian cells, we stably transfected N2A cells with a vector containing the full-length coding region of mouse Cx50 cDNA as described in Methods. Numerous clones surviving selection were picked and grown for additional studies; of these clones, clones 15, 17, 23 and 32 showed expression of mRNA with a size expected for the exogenous transcript (1·6 kb) as determined by Northern blot analysis. A representative Northern blot for Cx50 is shown in Fig. 1*A*, indicating that clone 17, clones 15 and 23, and clone 32 showed high, medium and low expression of Cx50 mRNA, respectively.

Expression of the Cx50 protein in two of the clones (clones 17 and 23) was evaluated by immunocytochemical techniques using an anti-Cx50 antibody (Fig. 1*B*). In many cells of both

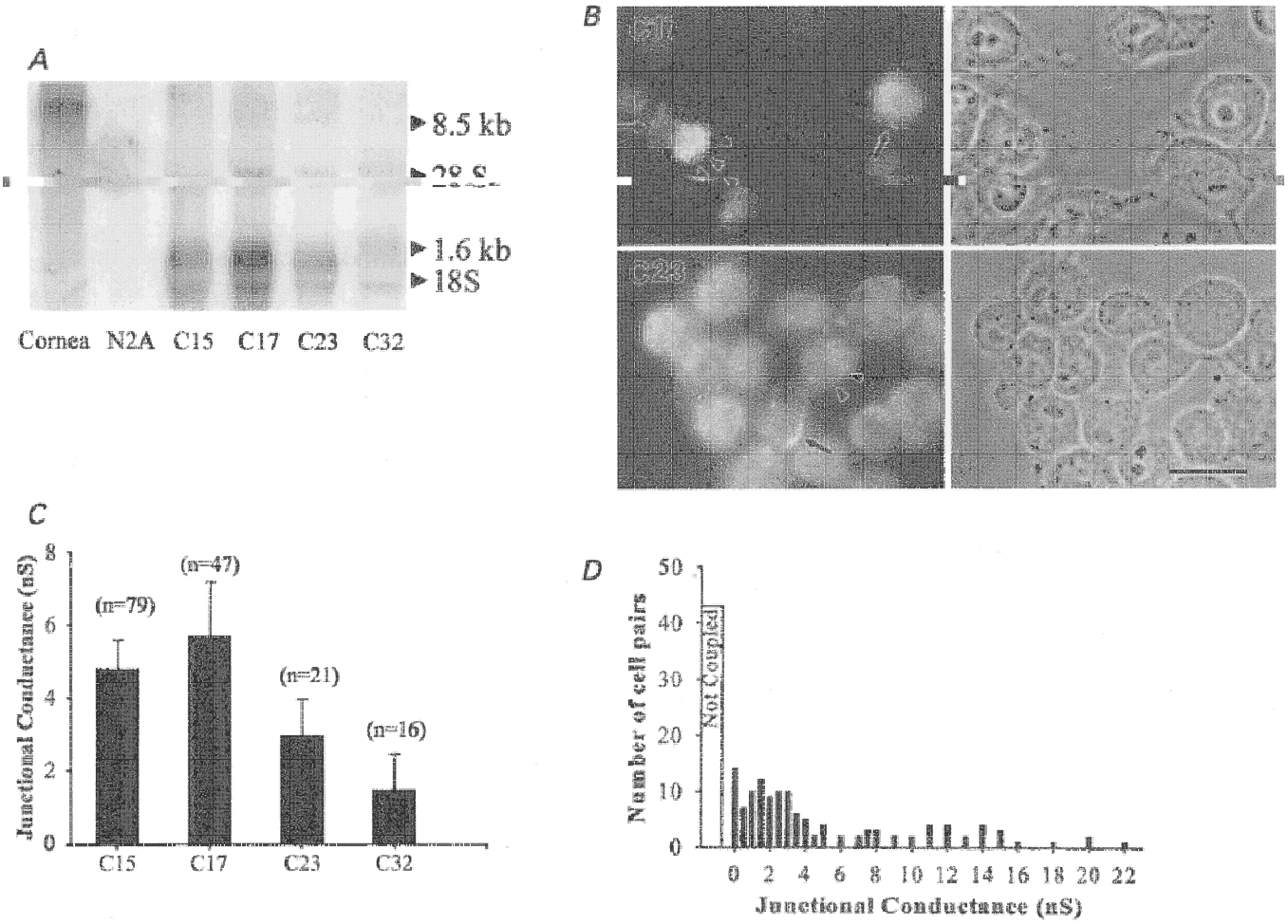

Figure 1. Molecular and functional expression of Cx50 in individual clones of N2A cells transfected with mouse Cx50 cDNA

A, Northern blots of wild-type corneal tissue, untransfected N2A cells and various clones (indicated by numbers below lanes) surviving selection following transfection of N2A cells with constructs containing the full-length coding sequence of mouse Cx50. ^{32}P probes generated using the entire coding region recognized a single mRNA species in several of the illustrated clones with apparent size (1·6 kb) as predicted for the construct. Expression of Cx50 mRNA was high in clones 15 and 17, moderate in clone 23 and low in clone 32. *B*, immunocytochemical analysis of Cx50 expression in clones 17 (top) and 23 (bottom) using an anti-Cx50 antibody. In both clones, punctate Cx50 staining was detected at appositions between cells (arrows) and at non-appositional regions (arrowheads). Phase contrast images are shown to the right and fluorescence micrographs to the left. Scale bar 25 μm. *C*, strength of electrical coupling in various clones. Junctional conductance values in the various clones are indicated as means + S.E.M. The magnitude of functional coupling roughly paralleled that of Cx50 expression. *D*, distribution of junctional conductance values measured between Cx50-transfected N2A cell pairs. Histogram shows maximum junctional conductances obtained in 120 cell pairs of Cx50 transfectants (clones 15 and 17) grouped in bins of 0·5 nS. The average conductance of coupled cell pairs transfected with Cx50 was 6·7 $\pm$ 2·6 nS.

clones, punctate Cx50 staining was detectable at appositions between cells as well as in non-appositional regions. The presence of such staining suggests that these transfectants express and successfully traffick this connexin to junctional regions.

In order to evaluate the strength of functional coupling, junctional conductance between cell pairs was determined using the dual whole-cell voltage clamp technique. The mean junctional conductance values in clones whose mRNA expression is illustrated in Fig. 1*A* (clones 15, 17, 23 and 32) were $4{\cdot}8 \pm 0{\cdot}8$ nS ($n = 79$), $5{\cdot}7 \pm 1{\cdot}5$ nS ($n = 47$), $2{\cdot}8 \pm 0{\cdot}7$ nS ($n = 21$) and $1{\cdot}5 \pm 1{\cdot}01$ nS ($n = 16$), respectively (Fig. 1*C*). Electrical coupling in highly expressing Cx50 clones was evident in greater than 60% of cell pairs. The maximum junctional conductance (g_j) in these clones ranged from 200 pS to 22 nS (Fig. 1*D*).

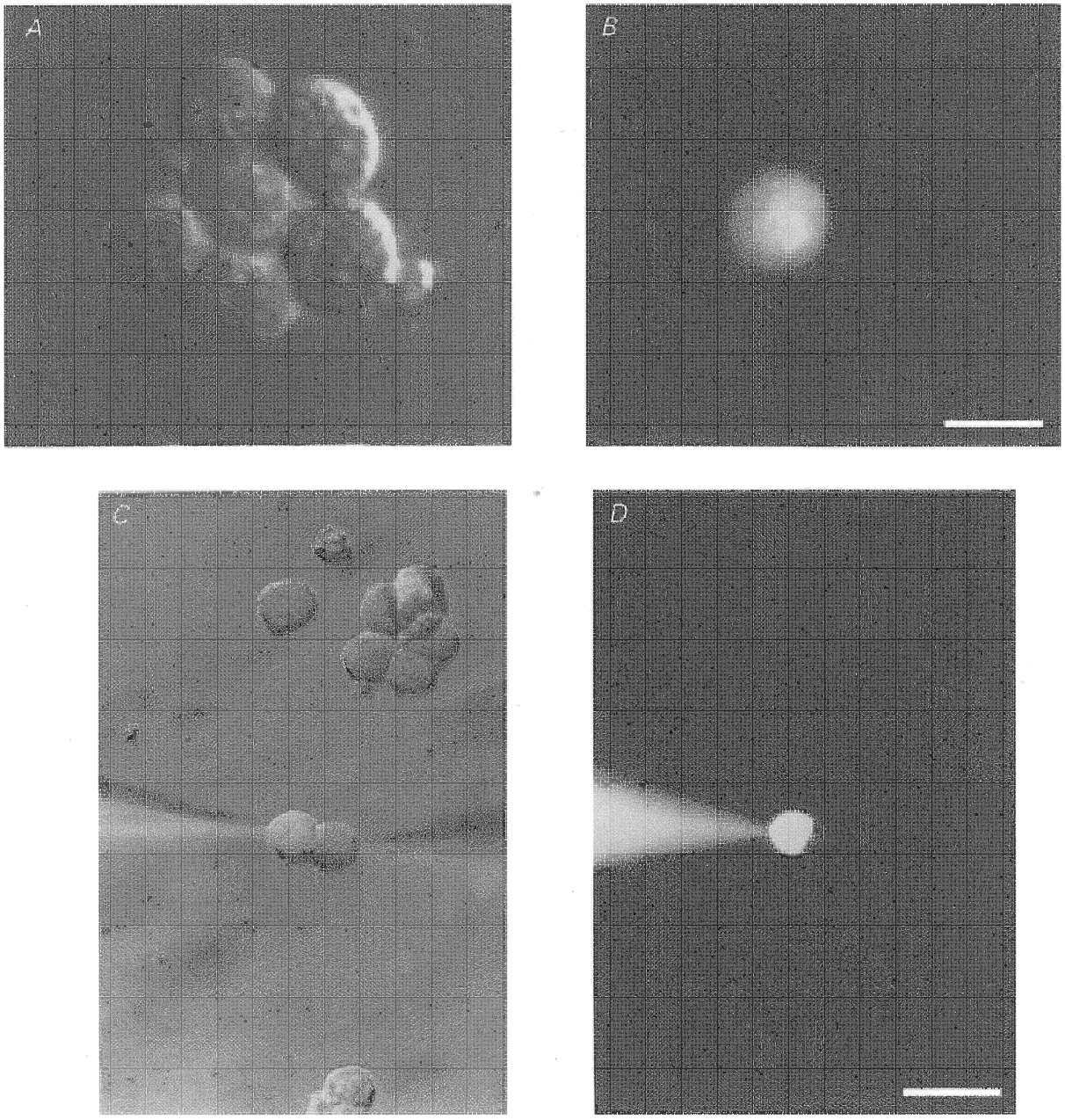

Figure 2. Lack of transfer of Lucifer Yellow dye in Cx50 transfectants

A and *B*, Lucifer Yellow dye was injected into the central cell of a cluster of Cx50-transfected cells through a microelectrode. Scale bar, 20 μm. *C* and *D*, lack of transfer of Lucifer Yellow evaluated in conjunction with the dual whole-cell voltage clamp technique in a cell pair in which the junctional conductance was 12 nS. Scale bar, 35 μm. Phase contrast images are shown in *A* and *C* and corresponding fluorescence micrographs in *B* and *D*. The fluorescence micrographs taken using FITC filters and xenon epi-illumination indicated minimal transfer of Lucifer Yellow.

Lucifer Yellow dye transfer

Functional coupling of Cx50-transfected cells was further characterized by evaluating the permeability of Cx50 channels to Lucifer Yellow, a highly fluorescent anionic dye with a molecular weight of 454 Da. Lucifer Yellow was injected into one cell of a cluster of N2A cells through a microelectrode and the spread of Lucifer Yellow into surrounding cells was monitored as described in Methods (Fig. 2*A* and *B*). In contrast to the high incidence of moderate to strong electrical coupling in cell pairs, spread of Lucifer Yellow dye was not detected in 86% of clusters of Cx50-transfected cells under these conditions (25 injections). For four injections, however, a low degree of dye transfer to one other cell was detected. Because junctional conductance was less than 2–3 nS in 48% of cell pairs, it was possible that the weak dye transfer reflected low values of junctional conductance. Therefore, in order to determine whether Lucifer Yellow spread was strictly correlated to junctional conductance (g_j), dye transfer in cell pairs was determined in conjunction with g_j measurements using the dual whole-cell voltage clamp technique (Fig. 2*C* and *D*). In these experiments Lucifer Yellow was added to one of the recording pipettes. Under these conditions, transfer of Lucifer Yellow was not detected even in those cell pairs where g_j was as high as 12 nS (Fig. 2*C* and *D*). Transfer of Lucifer Yellow was not observed in seven other cell pairs where whole-cell recordings revealed g_j values of 2, 4, 7, 10, 12, 14 and 15 nS. In some cell pairs, a low transfer of dye was detected when large positive gradients were imposed to facilitate the passage of the negatively charged dye. However, even under these conditions dye permeability was low and was observed only when g_j was higher than 20 nS. Together, these results indicate that Cx50 channels have a very low permeability to Lucifer Yellow.

Voltage sensitivity of Cx50 junctional conductance

To determine the sensitivity of junctional conductance (g_j) to transjunctional voltage (V_j) in Cx50-transfected cells, pulses of moderate duration (7–10 s) stepping from a holding potential of 0 mV to different voltages ranging from −100 to 100 mV (Fig. 3*A*, V_j traces) were applied to one cell of a

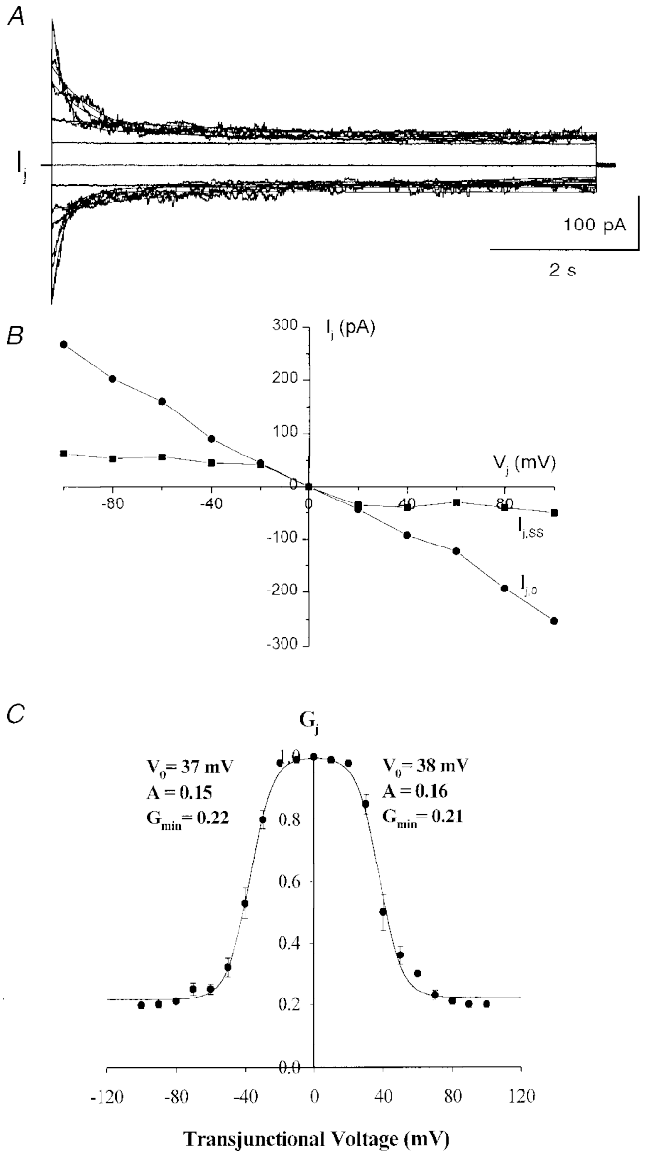

Figure 3. Dependence of junctional conductance of Cx50 gap junction channels on V_j

A, recordings of I_j measured in one cell of a pair in response to 8–10 s pulses from 0 to ±100 mV (in 20 mV increments) that were applied to the other cell. Junctional currents were maximal at the beginning of the pulses and declined to steady-state values in a time- and voltage-dependent manner when V_j exceeded ±20 mV. The continuous curves superimposed on the I_j traces are fits of the junctional current relaxations with monoexponential decay functions. *B*, current–voltage relationships for the instantaneous ($I_{j,0}$) and steady-state ($I_{j,ss}$) junctional currents, illustrating rectification of steady-state currents at $-20\ \text{mV} > V_j > 20\ \text{mV}$. In contrast, the instantaneous current remained linear throughout the entire voltage range (in this case the slope conductance was about 3 nS). *C*, relationship between V_j and steady-state junctional conductance of Cx50 gap junction channels. The normalized steady-state junctional conductance ($G_{j,ss}$, the ratio of the steady-state g_j to maximal g_j) at each voltage is shown; points represent means ± S.E.M. obtained in 10 experiments. The continuous line is a fit of the data to a two-state Boltzmann equation with parameters corresponding to each quadrant as indicated.

pair. The junctional currents (I_j) recorded from the unstepped cell declined from initial maximal values to steady-state values in a voltage- and time-dependent manner (Fig. 3*A*, I_j traces). Time-dependent decreases in I_j were clearly evident at V_js greater than +20 mV and lower than −20 mV (Fig. 3*A* and *B*). The instantaneous and steady-state junctional currents ($I_{j,0}$ and $I_{j,ss}$, respectively) plotted as a function of V_j are shown in Fig. 3*B*, clearly illustrating the voltage dependence of $I_{j,ss}$. The $I_{j,0}$–V_j relationship was found to be linear over the entire voltage range with a slope conductance of 3 nS in the illustrated case; in contrast, $I_{j,ss}$ showed rectification at $-20\ \text{mV} > V_j > 20\ \text{mV}$.

The dependence of the normalized steady-state g_j ($G_{j,ss}$) on V_j is shown in Fig. 3*C*. $G_{j,ss}$ was obtained by dividing the steady-state $I_{j,ss}$ by $I_{j,0}$ for each V_j. $G_{j,ss}$ data for V_js of each polarity were well described by a two-state Boltzmann relationship (eqn (1)). The best fit for the Boltzmann equation for the average $G_{j,ss}$ values (from 10 cell pairs; S.E.M. indicated for each $G_{j,ss}$ value) is shown as a continuous line. The following values for the Boltzmann parameters were obtained: $G_{min} = 0{\cdot}22$; $V_0 = -37$ mV; $A = 0{\cdot}15$ (gating charge = 3·7) for negative polarities and $G_{min} = 0{\cdot}21$, $V_0 = 38$ mV and $A = 0{\cdot}16$ (gating charge = 4) for positive polarities. These results indicate that Cx50 forms gap junction channels that are moderately sensitive to transjunctional voltage.

The relaxations of junctional currents during the course of the 7–10 s pulses were well described by single exponential functions (continuous lines superimposed on current traces in Fig. 3*A*) with time constants of decay that depended on the transjunctional voltage as illustrated in Fig. 4*A*. Time constants were largest (~4 s) at voltages near V_0 (30–40 mV) and declined to smaller values (minimally 100–200 ms) with increasing V_js of either polarity. Time constants of relaxation at negative and positive voltages were not significantly different. At very low V_j (10–20 mV), τ could not be accurately determined because of the absence of a measurable current decay. Therefore, in order to estimate τ, a prepulse to large V_j (90 or 100 mV) was first applied for 7 s and then the voltage was stepped to 10 or 20 mV; the time course of recovery of the junctional current at these voltages was used to estimate τ.

The description of the time course of junctional current relaxation in response to moderately long V_j pulses as a monoexponential process suggests that the underlying mechanism most probably consists of conversion between a single high conductance and a low conductance state. For such a two-state process, the rate constants at each voltage can be estimated from τ and the normalized steady-state conductance values ($G_{j,ss}$) according to the following equations (Harris *et al.* 1981):

$$\alpha = G_{j,ss}/\tau \text{ and } \beta = 1 - G_{j,ss}/\tau, \qquad (3 \text{ and } 4)$$

where α represents the rate constant for low-to-high conductance transitions and β is the rate constant for high-to-low conductance transitions. The values of α and β as a

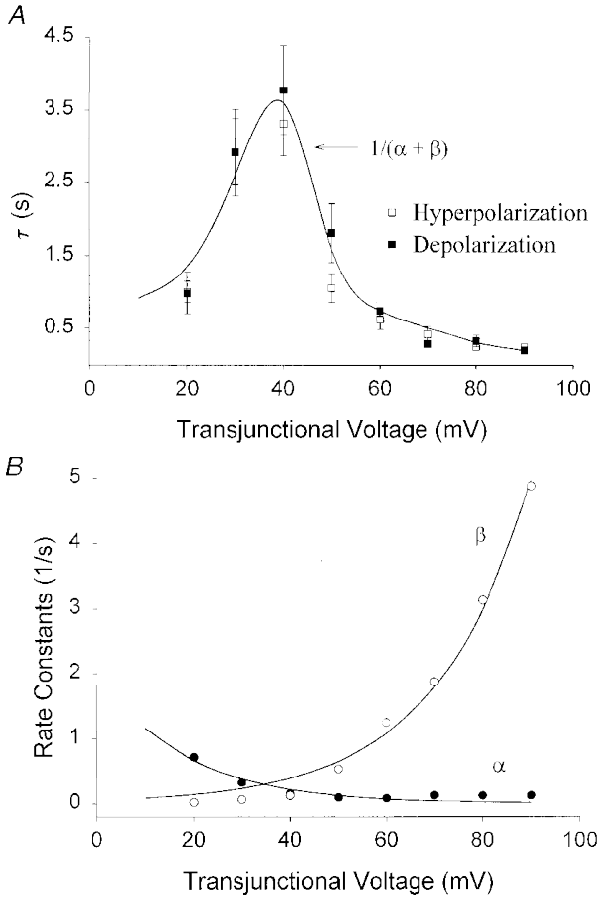

Figure 4. Voltage dependence of time and rate constants
A, time constants (τ) were determined from best fits of junctional current relaxations at positive and negative voltages from a total of 8 experiments. *B*, opening rate constant (α) and the closing rate constant (β) were determined at each voltage from the time constant values in *A* and the steady-state junctional conductance values presented in Fig. 4, using equations given in the text. The continuous lines in *A* and *B* are the best fits calculated from these equations.

function of the transjunctional voltage are shown in Fig. 4*B*. Both α and β were voltage dependent, with α predominating at low V_j and β predominating at higher voltages. Substituting in the above equations and defining a parameter k (the rate at which $\alpha = \beta$ reached at $V_j = V_0$), the relationship between rate constants and voltage can be described by:

$$\alpha = k \exp[-A_\alpha(V_j - V_0)], \quad (5)$$

and

$$\beta = k \exp[A_\beta(V_j - V_0)], \quad (6)$$

where A_α and A_β are the respective voltage sensitivities of

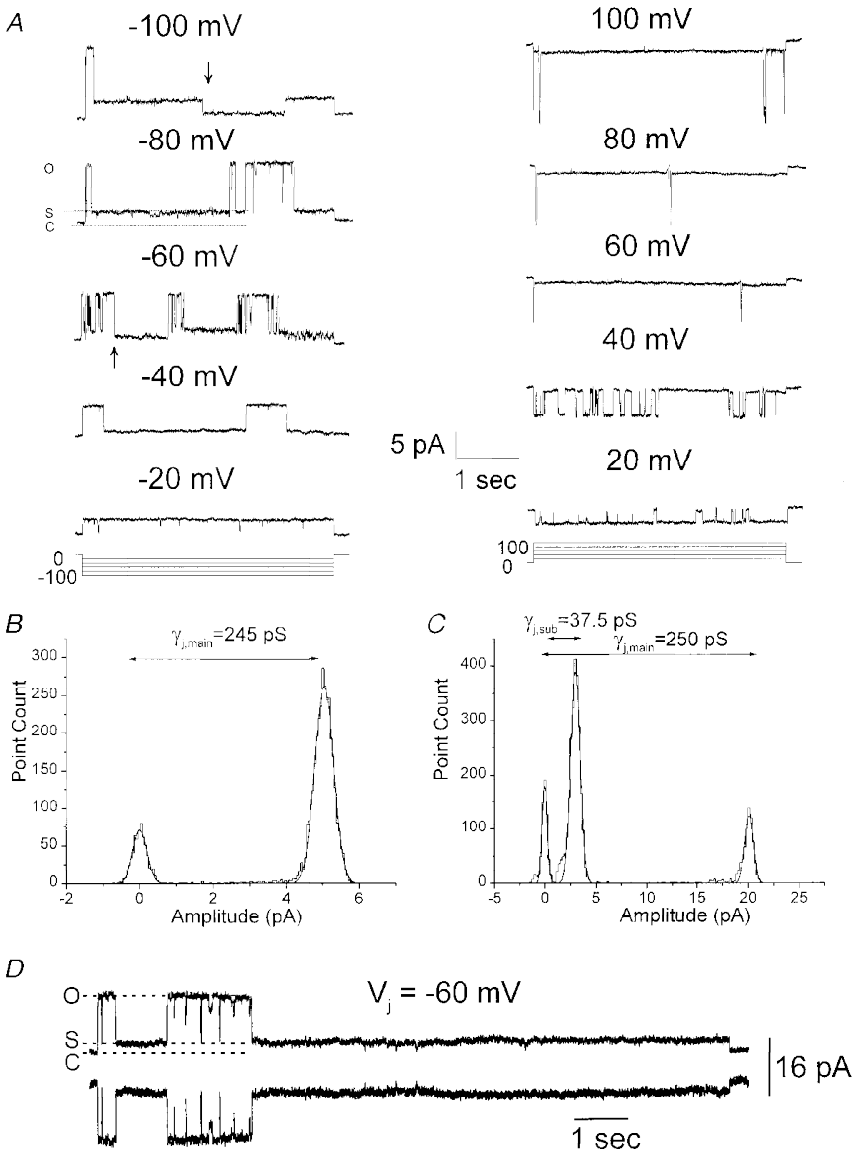

Figure 5. Unitary conductances of gap junction channels formed by Cx50 measured in a cell pair expressing a single channel with pipettes containing 130 mM CsCl

A, junctional currents measured in one cell of a Cx50-transfected N2A cell pair in response to 4 s voltage steps to −100 to +100 mV from a holding potential of 0 mV. Single Cx50 channels were maximally open (O) from the baseline level (C) immediately upon application of a voltage pulse, and junctional current exhibited transitions to a subconductance state (S) from the fully open state (O). These transitions were rapid and were clearly evident at V_js above 40 mV and below −40 mV. Transitions to the baseline level were rare; only two such transitions (arrows) were observed in the entire recording epoch. *B* and *C*, the all points amplitude histograms and corresponding fits to Gaussian functions for current recordings obtained at V_js of −20 (*B*) and −80 mV (*C*). The amplitude histogram in *B* has two peaks at 0 and 4·9 pA corresponding to a conductance of 245 pS for the fully open state. In *C*, three peaks at 0, 3·0 and 20 pA were observed, corresponding to the closed state, subconducting state and the fully open state, respectively. The peaks occurring at 0 pA for all points histograms at both V_js reflect the baseline current before application of pulse, and do not represent closed state currents during the pulse. *D*, single channel currents can be seen as simultaneously occurring equal sized events in both cells of a pair.

each rate constant (Harris *et al.* 1981). Best fits to experimental data occurred when $k = 0{\cdot}24$, $A_\alpha = 0{\cdot}054$, $A_\beta = 0{\cdot}072$ and $V_0 = 38$ mV. These parameters demonstrate that high-to-low conductance transitions were 1·3 times more sensitive to voltage than transitions from low-to-high conductance over the entire voltage range.

Lack of formation of functional Cx50 hemichannels

Some connexins (most notably wild-type Cx46 and Cx43 extracellular loop mutants exogenously expressed in *Xenopus* oocytes) have been reported to form functional hemichannels (connexons), that are activated maximally in low extracellular Ca^{2+} at depolarizing potentials (Paul *et al.* 1991; Ebihara & Steiner, 1993; Trexler *et al.* 1996). In order to determine whether the Cx50 protein forms functional hemichannels in mammalian transfectants, the whole-cell currents from single isolated cells in the absence and in the presence of external Ca^{2+} were measured in response to 8 s voltage pulses to −30 to 65 mV from a holding potential of 0 mV. Activation of hemichannel-like currents was not observed at depolarized potentials in 0 mM calcium. To further determine if cells expressing Cx50 gap junction channels formed functional hemichannels in 0 mM calcium, junctional conductance was first determined and then one cell of a pair was mechanically pulled away from the other cell. The non-junctional current measured in the two cells in 0 mM calcium was linear between −30 and 65 mV, suggesting a lack of hemichannel formation even in cells that strongly expressed Cx50 protein. Thus, on the basis of criteria used to define hemichannel activity in other cell types, Cx50 does not appear to form functional hemichannels in N2A cells.

Single channel conductances of Cx50 gap junction channels

Single channel conductance was measured from pairs of Cx50-transfected N2A cells soon after dissociation and replating, when there was a high incidence of weak functional coupling. Unitary current events were recognized as equal-sized events of opposite polarity that occurred simultaneously in each cell's current recording as illustrated in Fig. 5*D* for a cell pair at a V_j of 60 mV. Single channel currents in response to various V_j pulses between −100 mV and 100 mV in 20 mV increments are illustrated in Fig. 5*A*. Cx50 channels were always maximally open (O) above the zero current level (C) immediately upon application of V_j pulses. The amplitude histogram for the single channel current recorded at a V_j of −20 mV has a distinct peak at 4·9 pA that corresponds to the open channel level (Fig. 5*B*). The baseline current level (corresponding to the peak at 0 pA) before application and that after the end of the pulse are also illustrated for clarity. The amplitude histogram was fitted to a Gaussian function; the mean and variance of the unitary current were 0 pA and 0·97 pA for the baseline current and 4·9 pA and 1·2 pA for the open channel current indicating a single channel conductance ($\gamma_{j,main}$) of 245 pS.

Connexin50 channels frequently exhibited transitions to an intermediate conductance state (S) from the main conducting level (apparent in the single channel recording at $V_j =$

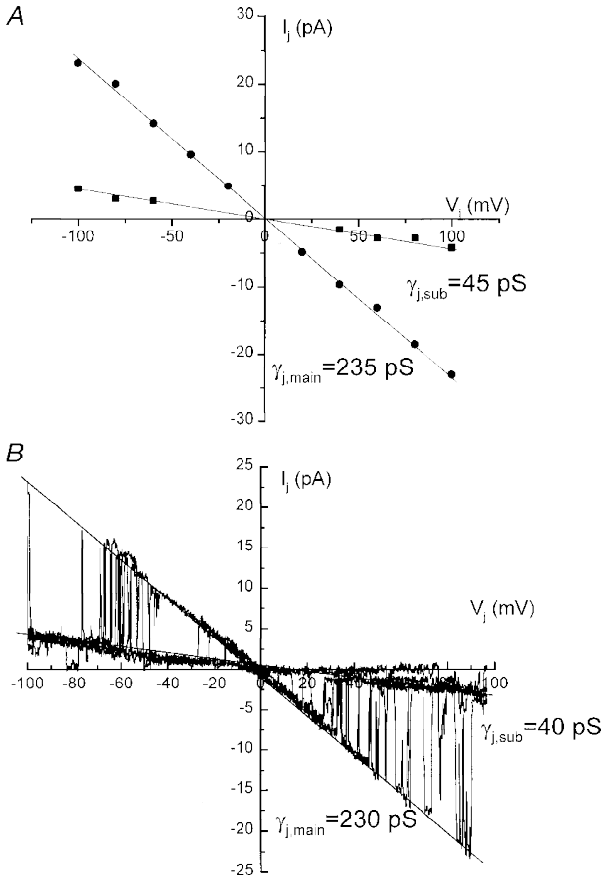

Figure 6. Single channel current–voltage (I_j–V_j) relationships of the junctional current constructed from responses of cells to voltage pulses or to a series of ramps from −100 to +100 mV

A, single channel current amplitudes of the fully open state and the subconductance state at each V_j measured from amplitude histograms for the recordings shown in Fig. 7. The unitary conductances of the fully open state ($\gamma_{j,main}$) and the subconductance state ($\gamma_{j,sub}$) obtained by linear regression (continuous lines) of the single channel I_j–V_j relationships were 235 and 45 pS, respectively. *B*, single channel current–voltage relationships constructed from the responses of junctional membrane to a series of ramps. The unitary conductance of the main state ($\gamma_{j,main}$) and the substate ($\gamma_{j,sub}$), measured as the slopes of the current–voltage relationships (continuous lines), were 230 and 40 pS, respectively.

−80 mV in Fig. 5*A* and in the all points amplitude histogram for this recording displayed in Fig. 5*C*). The gating of Cx50 channels to the intermediate conductance was clearly evident during V_j pulses above 20 mV and below −20 mV, and the concomitant presence of two distinct open levels was clearly evident at $-40 > V_j > 40$ mV. At these voltages, junctional currents exhibited direct interconverting transitions between the main open level (O), and the intermediate conductance level (S) level (Fig. 5*A*, most obvious in illustrated traces obtained at $V_j = -60$, −80 and −100 mV). Transitions between the two open levels were rapid and did not involve transitions to additional conductance states. Notably, the majority of the transitions at large voltages were between the main state and the subconductance state: transitions that involved the closed state (C), i.e. the baseline current, were very infrequent and did not occur in a consistently voltage-dependent manner. In the illustrated series of pulses only two such transitions were observed, and both occurred at large voltages (arrows marking such events in −60 mV and −100 mV traces in Fig. 5*A*). The all points amplitude histogram of the single channel current at a V_j of −80 mV has two distinct peaks at 3·0 and 20 pA (variances of Gaussian fits are 2·3 and 2·0 pA, respectively) corresponding to the intermediate conductance state (37·5 pS) and the fully open state (250 pS), respectively (Fig. 5*C*). The peak at 0 pA represents the baseline current before application of the pulse.

The single channel I_j–V_j relationship for this particular cell pair is shown in Fig. 6*A*. The single channel conductances of the fully open state and the subconductance state of Cx50 channels, obtained by linear regression of the single channel *I*–*V* relationships, were 235 and 45 pS, respectively. Single channel currents for the two open states were also obtained from amplitude histograms that were compiled from 60 s pulses (see Fig. 7). Linear regressions of single channel current–voltage relationships yielded values of 230 and

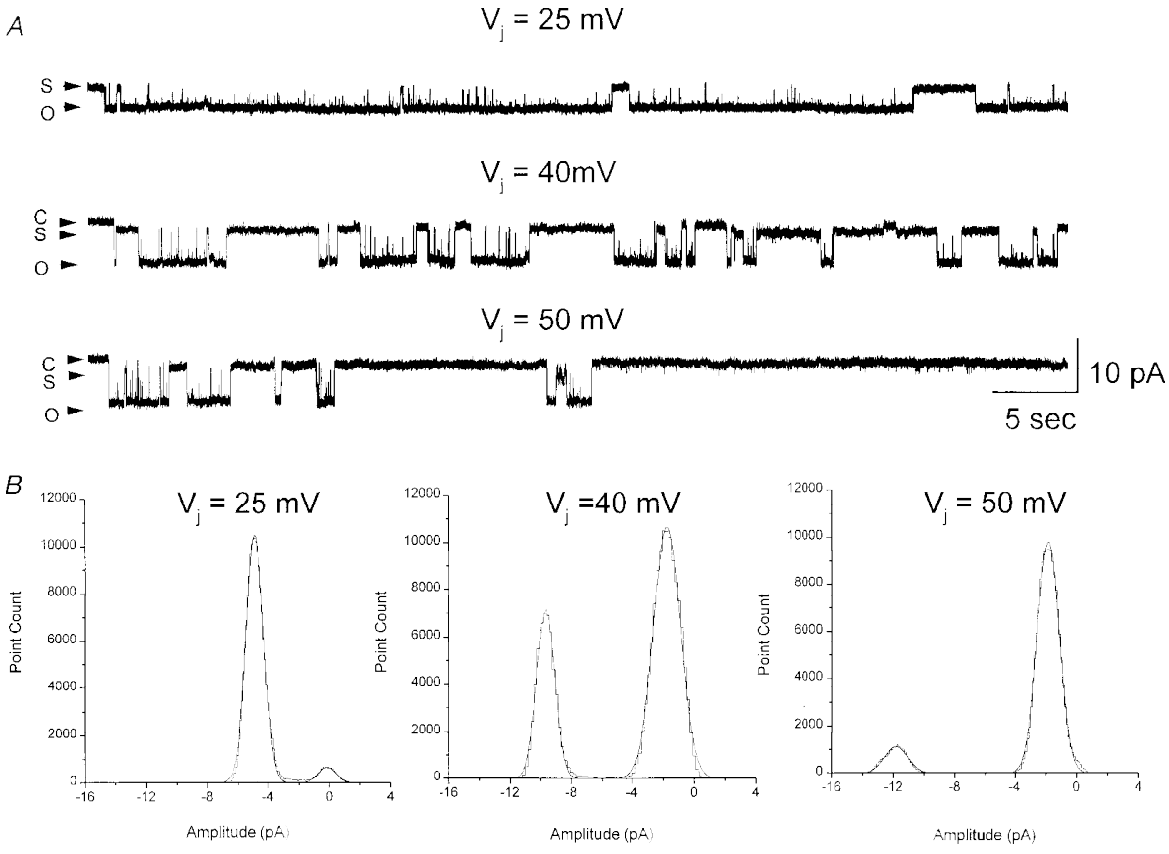

Figure 7. Unitary junctional currents illustrating the dependence of open probability on the transjunctional voltage

A, single channel junctional currents recorded at transjunctional voltages of 25 mV (top), 40 mV (middle) and 50 mV (bottom). The first 60 s of 2–4 min recordings at 40 and 50 mV are displayed; the current trace at 25 mV is displayed 70 s after application of the pulse from a 6 min long recording. Dwell times in the open state (O) decreased with increasing voltages, whereas residence in subconductance state (S) was found to be favoured at higher voltages. Current traces were filtered at 200 Hz and sampled at 2 kHz. *B*, all points amplitude histograms of the recordings have two distinct peaks for each V_j pulse, corresponding to the fully open state and the residual subconductance state. The area under the peak corresponding to the fully open state decreased with increasing V_j, whereas the area corresponding to the subconductance state increased with increasing V_j.

Table 1. Calculation of P_o from multichannel recordings

Cell pair	V_j (mV)	N	Level occupation probabilities					Δ	P_o
			P_0	P_1	P_2	P_3	P_4		
1	+40	2	54·7	43·0	2·7	—	—	14·6	0·25
	−30	2	15·9	50·1	34·0	—	—	4·5	0·59
2	+50	5	35·5	38·2	19·1	6·4	4·8	2·15	0·22
	+35	5	16·5	31·7	21·7	13·2	10·8	2·80	0·35
3	+35	3	22·9	41·4	28·2	7·6	—	2·7	0·4
4	−30	2	40·6	57·5	1·8	—	—	27·7	n.f.
	+40	2	59·0	35·7	5·3	—	—	4·1	0·23
5	+20	2	1·8	25·5	72·7	—	—	1·4	0·85
	+25	2	20·5	54·0	31·6	—	—	4·5	0·60
	+30	2	7·2	41·4	52·6	—	—	4·5	0·73
	+40	2	53·8	40·1	6·1	—	—	4·9	0·26
6	+50	2	91·8	6·6	1·6	—	—	0·29	n.f.
	+30	2	29·2	37·1	33·7	—	—	1·4	n.f.
7	+20	2	3·6	40·5	55·8	—	—	7·96	0·75
	−30	2	14·8	46·8	38·4	—	—	3·8	0·65
8	+40	2	91·6	6·0	2·4	—	—	1·12	n.f.
	−40	2	77·5	24·1	5·9	—	—	1·4	0·58

N, maximum number of open channels observed during the recording; $\Delta = P_1^2/P_0 \times P_2$ as defined by Manivannan *et al.* (1992); P_o, open probability calculated by fitting the level occupation probabilities to the binomial equation; n.f., data was not a good fit ($r^2 < 0·7$) to the binomial equation.

41 pS (data not shown) for the fully open state and the subconductance state, respectively. The mean single channel conductance of Cx50 channels was $220 \pm 13·1$ pS ($n = 12$) for the fully open state and $43 \pm 4·2$ pS ($n = 10$) for the subconductance state.

The gating of Cx50 channels between the fully open state and a subconductance state was also evident in experiments where junctional current through a single Cx50 channel was determined in response to voltage ramps from −100 to +100 mV (Fig. 6*B*). The single channel currents exhibited transitions between the main state, that was favoured at low voltages, and the subconductance state, that was favoured at high voltages. The main state and substate conductances determined as the slopes of the current–voltage relationships during the voltage ramps were 230 and 40 pS, respectively.

Open probability as a function of V_j

Visual inspection of the records of Fig. 5*A* and comparison of the amplitude histograms obtained from V_j pulses of −20 mV and −80 mV (Fig. 5*B* and *C*) indicated that the dwell times in the main open level decreased at large voltages, suggesting a decrease in P_o. To determine the dependence of the P_o of Cx50 channels on transjunctional voltage, channel activity was recorded for long durations (1–4 min) (Fig. 7). The initial 60 s segments of long single channel recordings

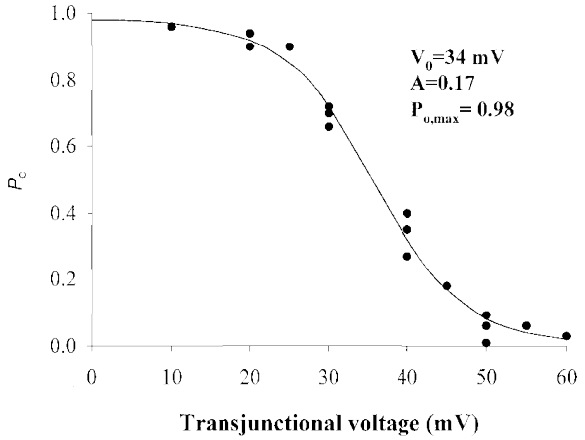

Figure 8. Dependence of open probability (P_o) on the transjunctional voltage

P_o was determined as the fraction of time spent in the fully open state between 20 and 60 s after application of the pulse. Each point represents one single determination; P_o values were determined from a total of 4 cell pairs in which a single channel was active. Continuous lines are the best fit of the data to the Boltzmann equation:

$$P_o = P_{o,max}/\{1 + \exp[A(V_j - V_0)]\}.$$

The values of the parameters are listed in the text.

from a cell pair obtained at V_j pulses of 25, 40 and 50 mV are shown in Fig. 7. At a V_j of 25 mV, single Cx50 channels resided predominantly in the fully open state, with frequent transitions to the lower conductance state. At voltages near V_0 (40 mV), residence in the fully open state became less frequent and at even higher voltages (50 mV), Cx50 channels resided predominantly in the residual subconductance state. The decrease in P_o with increasing V_js is clearly evident in amplitude histograms of the current records compiled from the first 60 s after application of V_j pulses (Fig. 7*B*). Histograms show two distinct peaks at each V_j pulse, corresponding to the residual subconductance state and the fully open state. These peaks are at −4·9 and −0·6 pA at a V_j of 25 mV, at −9·7 and −1·76 pA at a V_j of 40 mV and at 11·8 and −2·1 pA at a V_j of 50 mV. The proportion of the time spent in the fully open state at 25, 40 and 50 mV was 0·90, 0·35 and 0·1, respectively.

The dependence of P_o on the transjunctional voltage obtained early during the application of long duration pulses to cell pairs displaying a single functional channel is shown in Fig. 8. Each point represents a single determination from a total of four cells where the P_o of the channel was estimated as the fraction of time spent in the fully open state. The $P_o - V_j$ relationship was well described by a Boltzmann relationship (continuous curve, Fig. 8). The best fit of the data was obtained when $V_0 = 34$ mV, $A = 0{\cdot}17$ (gating charge = 4·5) and maximum P_o ($P_{o,max}$) = 0·98.

Channel open probability was also estimated from multichannel recordings using previously described procedures (Manivannan *et al.* 1992). Table 1 shows level occupation probabilities (P_0, P_1,...) at various V_j values for eight cell pairs determined from the fits of amplitude histograms to Gaussian functions. P_o was calculated from the fits of these values to the binomial equation (Table 1). Although there was a considerable variability in P_o values, the general trend was a decrease in P_o as V_j increased. In order to distinguish between co-operative gating in Cx50 channels, Δ values were calculated for each recording. Δ values ranged from 0·29 to 27·7 for cell pairs that contained two to four Cx50 channels, suggesting the presence of both independent (similar and identical) and co-operative interactions between channels according to previously defined criteria (Manivannan *et al.* 1992). In cell pairs with two active channels ($N = 2$) an accurate fit of the occupation probabilities to the binomial equation was not obtained in 4 of 14 recordings; in such instances, the Δ value was less than 4, implying a co-operative interaction between channels (Manivannan *et al.* 1992; Ramanan & Brink, 1993). In all other recordings, the Δ value was consistent with the presence of independent channels that were either identical ($2 < \Delta < 4$ when $N > 2$, or $\Delta > 4$ when $N = 2$) or similar ($\Delta > 4$ when $N > 2$). For example, the Δ value for cell pair 4 was 27·7, and an accurate fit to the binomial equation was not obtained, suggesting that in this particular case channel open probabilities were most likely to be similar, not identical.

Ensemble currents

In order to establish that the decline of the macroscopic junctional current is due to the ensemble activity of identical and independent channels exhibiting transitions between

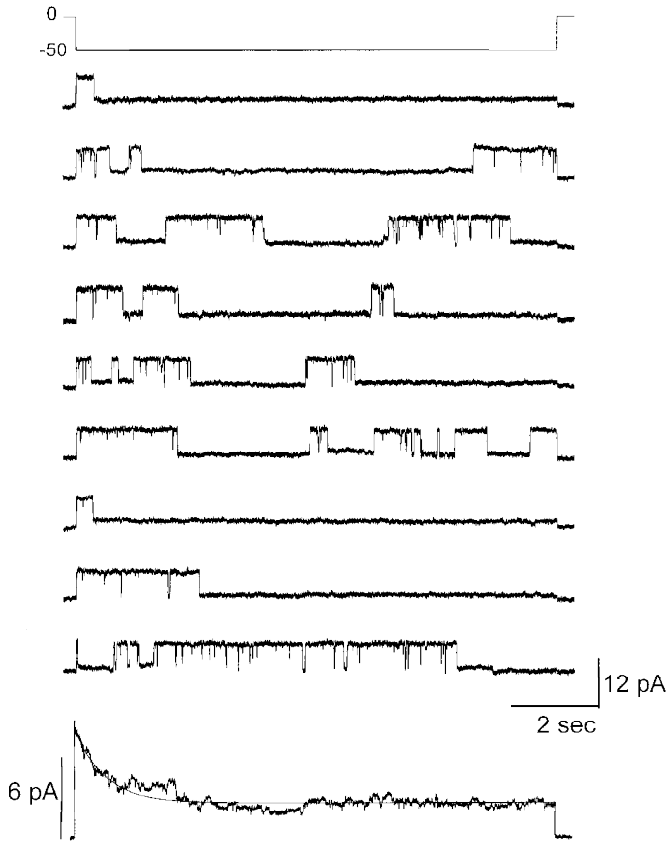

Figure 9. Unitary junctional currents in response to a series of consecutive 10 s pulses to a V_j of −50 mV and the resulting ensemble average current obtained from 35 such pulses (bottom)

V_j pulses to −50 mV were applied every 34 s. The ensemble average current declined in a monoexponential manner with a time constant of 905 ms, a value that is similar to the decline of the macroscopic current at the same voltage (Fig. 4).

the fully open state and the subconductance state, the ensemble average current of single Cx50 channels was determined. Shown in Fig. 9 are single channel currents in response to consecutive pulses to a V_j of −50 mV. Single channel currents in almost all cases exhibited transitions between the fully open state and a subconductance state. The average ensemble current during the course of the 10 s pulse obtained from 35 such pulses declined in a mono-exponential manner with a time constant of 905 ms (bottom record, Fig. 9), a value that is close to the macroscopic current decline at a V_j of −50 mV. Similar results were obtained in three other cell pairs that were subjected to consecutive pulses to V_js between −60 and −80 mV. These results clearly indicate that the macroscopic current after short pulses is due to the stochastic opening and closing of independent and identical Cx50 channels.

Ionic selectivity

In order to initially characterize the ionic selectivity of Cx50 channels, single channel conductances were measured under conditions where CsCl was replaced with equimolar concentrations of KCl or potassium glutamate (Fig. 10*A* and *B*, respectively). A similar approach has been used to assess the selectivity of gap junction channels formed of various other connexins (Veenstra, 1995; Beblo & Veenstra, 1997). Unitary current amplitudes in response to sustained V_j = −50 mV in KCl- and potassium glutamate-containing patch pipettes were 9·8 and 8·6 pA, respectively, corresponding to single channel conductances of 196 and 172 pS (Fig. 10*A* and *B*). The average single channel conductances in KCl and potassium glutamate obtained from linear regression of single channel currents were 195 ± 8 (n = 5) and 172 ± 6·5 (n = 4), respectively (Fig. 10*C* and *D*). Similar single channel

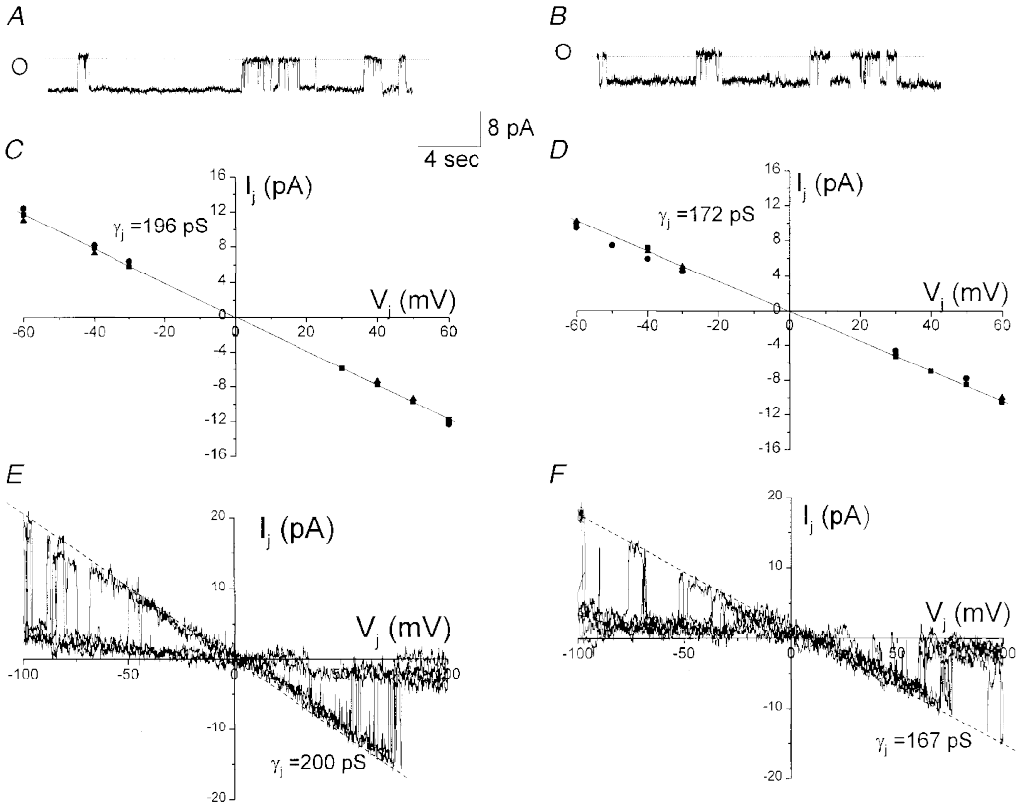

Figure 10. Ionic selectivity of Cx50 channels

A and *B*, unitary junctional currents of Cx50 channels recorded using 130 mM KCl (*A*) or potassium glutamate (*B*) internal solutions in response to voltage pulses of 50 mV (*A* and *B*). The amplitudes of junctional currents at 50 mV were 9·8 and 8·6 pA in KCl and potassium glutamate, respectively. *C* and *D*, single channel current amplitudes of the fully open state at each V_j were measured from amplitude histograms obtained with 130 mM KCl (*C*) and 130 mM potassium glutamate (*D*). The unitary conductances of the fully open state (γ_j) in KCl and potassium glutamate obtained by linear regression (continuous lines, $r^2 = 0{\cdot}94$ and 0·97, respectively) of the single channel I_j–V_j relationships were 196 and 172 pS, respectively. *E* and *F*, single channel current–voltage relationships constructed from the responses of junctional membrane to a series of consecutive V_j ramps (100 to −100 mV). The unitary conductance of the main state (γ_j) in 130 mM KCl (*E*) and 130 mM potassium glutamate (*F*), measured as the slopes of the current–voltage relationships, were 200 and 167 pS, respectively. The ratio of the conductance of Cx50 channels using potassium glutamate and KCl internal solutions ($\gamma_{j,Kglut}/\gamma_{j,KCl} = 0{\cdot}87$) is not as predicted by the ratio of ionic mobilities ($D_{Kglut}/D_{KCl} = 0{\cdot}36$), suggesting a lower permeability of these channels to anions. Current traces were filtered at 100 Hz and sampled at 1 kHz.

conductances using these internal solutions were calculated from currents measured during the application of V_j ramps from −100 to +100 mV (Fig. 10*E* and *F*).

The Goldman–Hodgkin–Katz equation predicts a 36% decrease in the single channel conductance when chloride ions are replaced by a lower mobility ion such as glutamate, assuming that the permeabilities of all monovalent ions are directly proportional to their respective aqueous mobilities (see Hille (1992). In our experiments, we found only a 14% decrease in the single channel conductance when potassium glutamate replaced KCl. These results suggest that Cx50 forms gap junction channels that are selective for cations over anions.

DISCUSSION

We have stably transfected communication-deficient N2A cells with the full-length DNA coding sequence for Cx50 and characterized the biophysical properties of moderate- and low-expressing clones. The results of this study demonstrate that Cx50 gap junction channels have a large single channel conductance (main state $\gamma_j > 200$ pS), are strongly sensitive to transjunctional voltage with first-order kinetic processes governing voltage sensitivity, and are more permeable to cations than to anions. In addition, transfer of the negatively charged dye Lucifer Yellow was only rarely detected even in very well coupled Cx50 transfectants. In contrast to *Xenopus* oocyte expression experiments in which the other lens connexin Cx46 was found to form functional hemichannels, our studies of Cx50-transfected N2A cells under conditions of low extracellular Ca^{2+} failed to reveal such non-junctional currents. These results define the properties of one of the lens connexins and provide the groundwork for exploring the role of gap junctions in lens function and for using site-directed mutagenesis to determine the functional consequences of amino acid substitutions in the Cx50 sequence which are reportedly associated with cataract formation (Steele *et al.* 1997; Shiels *et al.* 1998).

Unitary conductance of Cx50 gap junction channels

Unitary conductance of Cx50 channels was measured in transfected clones where expression of Cx50 and its mRNA were low to moderate and in more highly expressing clones soon after cell dissociation and replating, when functional coupling was low (Moreno *et al.* 1991*b*). Unitary junctional conductances (γ_js) were measured from cell pairs exhibiting one or two open channels using both voltage ramp protocols and long voltage step protocols. γ_j was found to exhibit a fully open state ($\gamma_{j,main}$) of about 220 pS (using 130 mM CsCl as internal solution) favoured at low V_j values and a residual or substate γ_j value ($\gamma_{j,sub}$) of 45 pS whose occupancy was favoured at V_j values beyond ± 40 mV. The ratio $\gamma_{j,sub}/\gamma_{j,main}$ (= 0·2), corresponds well with the ratio g_{min}/g_{max} obtained from macroscopic g_j measurements, thus providing further support for the proposal that the residual conductance g_{min} seen at high V_j arises from channel transitions occurring from the main state to the residual subconductance state (Moreno *et al.* 1994*a*; Bukauskas *et al.* 1995).

Unitary conductance measurements of mammalian gap junction channels stably expressed in mammalian cells range from 30 pS (human and chick Cx45: Veenstra *et al.* 1994; Moreno *et al.* 1995) to 300 pS (human Cx37: Reed *et al.* 1993). Within this range, the unitary conductance of rat Cx40 (with γ_j ~200 pS) is most similar to the results reported here for Cx50 (Traub *et al.* 1994; Hellmann *et al.* 1996). Channel activity with unitary conductances in this range has been reported in adult rabbit atrial myocytes (Verhule *et al.* 1997) and in a cell line derived from chorionic carcinoma cells (Hellmann *et al.* 1996) where it was attributed to Cx40, and in differentiating lens cells in culture (Donaldson *et al.* 1995) where it presumably represents Cx50 expression. Whether other channel sizes reported in the lens cells represent transitions between the states of Cx50 channels or represent the presence of other lens connexins will require further studies.

Voltage sensitivity of Cx50 gap junction channels

Macroscopic measurements using moderately long V_j pulses indicated that current flow through gap junction channels formed of Cx50 responded with monoexponential declines to steady-state levels that appeared to be complete within the initial 10 s of the pulse. The extent of total decline in I_j increased as V_j increased, although even at very high V_j values (± 100 mV), a residual I_j remained. After subtraction of residual conductance (g_{min}), steady-state g_j was fitted well by a form of the two-state Boltzmann equation, where the distribution of events in two states is dependent on the energy difference between them. As discussed below, these two states appear to be the fully open channel state (O) and the residual conductance state (S). Values for the Boltzmann parameters obtained from macroscopic measurements were $V_0 = \pm 38$ mV, gating charge = 4 and $g_{min}/g_{max} = 0{\cdot}21$; parameters obtained for positive and negative V_js were virtually identical, indicating that Cx50 channels are insensitive to inside-outside voltage ($V_{i\text{-}o}$). The calculated energy difference between the two states ($A\,V_0$: Harris *et al.* 1981) is 5·5–6·1 kcal mol^{-1}.

Boltzmann parameters have been determined for several other connexins expressed in *Xenopus* oocytes and in mammalian cell lines. Values range from $V_0 = 60$, gating charge = 2·5 and $g_{min}/g_{max} = 0{\cdot}37$ for Cx43, the least voltage-sensitive gap junction channel thus far characterized, to $V_0 = 14$ mV, gating charge = 2·4 and $g_{min}/g_{max} = 0$ for the gap junction channel expressed in cultured rat Schwann cells (Chanson *et al.* 1993), the most voltage-sensitive mammalian gap junction channel known. Thus, Cx50 channels form channels with a stronger sensitivity to transjunctional voltage than most connexins that have been characterized to date. Notably, the voltage sensitivity described for Cx50 in this study is markedly lower than that reported for Cx50 expressed in *Xenopus* oocytes

($V_0 = 18$ mV, gating charge = 8·5, $G_{min}/G_{max} = 0{\cdot}14$: White *et al.* 1994). Differences in voltage sensitivity for other connexins when expressed in oocytes and in mammalian cells has been noted previously, but in all other cases, the voltage sensitivity in mammalian expression systems is steeper than in oocytes. Whether differences in voltage sensitivity of Cx50 results from differences in post-translational processing of the gap junction protein in these systems warrants further investigation.

The kinetics of decline in macroscopic current during moderately long (7–10 s) pulses were evaluated in order to derive rate constants for transition between O and S. Time constants for current relaxations varied from maximal values of 3–4 s at 40 mV to 100–200 ms at 100 mV; no significant difference was found between I_j responses to V_j pulses of positive and negative polarity. Rate constants derived from the $G_{j,ss}$–V_j relationship and the τ–V_j relationship indicated that the closing rate constant (β) was 1·3 times more voltage sensitive than the opening rate constant (α). Voltage sensitivity of α and β have been calculated for gap junctional channels formed of Cx32 (Moreno *et al.* 1991*a*), Cx45 (Moreno *et al.* 1995; Barrio *et al.* 1997) and the Schwann cell connexin (Chanson *et al.* 1993). In all cases, the voltage sensitivity of β was greater than that of α, with A_β/A_α ranging from 1·4 to 2; the values for Cx50 channels are consistent with these results.

Voltage sensitivity of Cx50 evaluated in weakly coupled cell pairs

Channel gating at the microscopic level was assessed by measurements of channel open probability (P_o) as a function of V_j. For recordings where only one channel was present and where junctional current during the first 20–60 s of the recording was analysed, P_o of the main state was well described by a two-state Boltzmann equation with $V_0 =$ 34 mV, $A = 0{\cdot}17$ and $P_{o,max} = 0{\cdot}98$. Although occupancy of the residual or subconductance state could not be resolved at low driving forces, estimates of P_o for the subconductance state ($P_{o,sub}$) are virtually 1 at all V_j values above 60 mV. The close agreement between steady-state parameters of voltage sensitivity obtained from macroscopic and single channel recordings strongly indicates that, at early times after an imposed V_j, the steady-state conductance is determined by the ensemble activity of independent gap junction channels. Calculations of P_o from multichannel data also revealed that P_o decreased at high V_j values. Manivannan *et al.* (1992) used the parameter Δ ($= P_1^2/P_0P_2$) to distinguish between activity of identical or similar independent channels and of co-operative channels. For the case where there are only two channels, the condition $\Delta < 4$ was proposed to indicate the presence of co-operative interaction (Manivannan *et al.* 1992). Our analysis of multichannel data indicated that in four of six cell pairs with two active channels the Δ value was more than 4. In addition, in the other two recordings with three or five active channels, the Δ value ranged from 2·15 to 27·7 suggesting the presence of both identical and similar independent channels (Mannivannan *et al.* 1992). These values satisfy the criteria proposed by Manivannan *et al.* (1992) for independence and indicate that, in the majority of cases, voltage gating of Cx50 channels is non-co-operative.

Transitions between O and S predominate during the initial 7–60 s of a V_j pulse and may thus fully account for the voltage-dependent relaxation of junctional currents observed in macroscopic recordings from which the rate constants α and β were determined (see Vogel *et al.* 1998). Several lines of evidence indicate that the macroscopic voltage sensitivity of Cx50 gap junctions in response to short pulses appears most likely to be due to the ensemble activity of a homogeneous population of independently gated channels. First, macroscopic junctional currents declined monoexponentially from instantaneous to steady-state levels, as would be expected for a first-order process operating on independent channels. Second, the steady-state voltage sensitivity observed for single channel currents in cell pairs exhibiting only one channel is described well by Boltzmann parameters that are virtually identical to those that best fit the macroscopic data. (In the simple scheme described above with independently gated channels underlying the macroscopic voltage sensitivity, both P_o and the voltage-sensitive component of g_j ($G_{max} - G_{min}$) should be proportional to $\alpha/(\alpha + \beta)$.) Third, the ensemble average current obtained from 25 consecutive pulses to various V_j pulses declined with a time constant that was similar to the macroscopic current decline at the same voltages. Fourth, multichannel occupational probability data evaluated according to the criteria of Manivannan *et al.* (1992) revealed that in the majority of cases this behaviour was as expected for a homogeneous and non-co-operative population. Finally, it should be noted that the ratio of main state-to-substate single channel conductances closely approximates the ratio G_{min}/G_{max}; this close approximation is predicted from the ensemble action of independent channels with $P_o \sim 1$ at low voltages and $P_{o,s} \sim 1$ at high voltages.

Ionic selectivity

Ion substitution experiments on gap junction channels formed by other connexins have revealed that each channel type exhibits a unique anion : cation permeability ratio (Veenstra *et al.* 1994, 1995). Our quantitative studies on Cx50 channels, although thus far confined to a comparison of KCl and potassium glutamate, indicate a clear preference of the channel for permeation by cations. In addition, Cx50 channels were poorly permeable to Lucifer Yellow; when measured simultaneously with junctional conductance, such diffusion only occurred at very high g_j values. The low permeability of Cx50 channels to Lucifer Yellow may be explained by the high cation selectivity of these channels, although diffusion of the dye may also be limited by its large size. Nevertheless, such low permeability to anions suggests that these channels would be poorly permeable to second messenger molecules such as cAMP and IP_3, which are of

sizes similar to that of Lucifer Yellow. In the lens, where the most likely role of gap junction is metabolite exchange between fibre cells and between epithelial and fibre cell compartments, it is conceivable that such low anion permeability of Cx50 channels necessitates the expression of an additional connexin between the fibre cells.

Barrio, L. C., Capel, J., Jarillo, A. C., Castro, C. & Revilla, A. (1997). Species-specific voltage-gating properties of connexin45 junctions expressed in *Xenopus* oocytes. *Biophysical Journal* **73**, 757–769.

Barrio, L. C., Suchyna, T., Bargiello, T., Xu, L. X, Roginski, R. S., Bennett, M. V. L. & Nicholson, B. J. (1991). Gap junctions formed by connexins 26 and 32 alone and in combination are differently affected by applied voltage. *Proceedings of the National Academy of Sciences of the USA* **88**, 8410–8414.

Beblo, D. A. & Veenstra, R. D. (1997). Monovalent cation permeation through the connexin40 gap junction channel Cs, Rb, K, Na, Li, TEA, TMA, TBA and effects of anions Br, Cl, F, acetate, aspartate, glutamate, and NO_3. *Journal of General Physiology* **109**, 509–522.

Bennett, M. V. L., Barrio, L. C., Bargiello, T. A., Spray, D. C., Hertzberg, E. & Saez, J. C. (1991). Gap junctions: new tools, new answers, and new questions. *Neuron* **6**, 305–320.

Bruzzone, R., White, T. W. & Paul, D. L. (1996). Connections with connexins: the molecular basis of direct intercellular signalling. *European Journal of Biochemistry* **238**, 1–27.

Bukauskas, F. F., Elfgang, C., Willecke, K. & Weingart, R. (1995). Biophysical properties of gap junction channels formed by mouse connexin40 in induced pairs of transfected human HeLa cells. *Biophysical Journal* **68**, 2289–2298.

Chanson, M., Chandross, K. J., Rook, M. B., Kessler, J. A. & Spray, D. C. (1993). Gating characteristics of a steeply voltage-dependent gap junction channel in rat Schwann cells. *Journal of General Physiology* **102**, 925–946.

Dermeitzel, R., Hertzberg, E. L., Kessler J. A. & Spray, D. C. (1991). Gap junctions between cultured astrocytes: immunocytochemical, molecular and electrophysiological analysis. *Journal of Neuroscience* **11**, 1421–1432.

Donaldson, P. J., Dong, Y., Roos, M., Green, C., Goodenough, D. A. & Kistler, J. (1995). Changes in lens connexin expression lead to increased gap junctional voltage dependence and conductance. *American Journal of Physiology* **269**, C590–600.

Eghbali, B., Kessler, J. A. & Spray, D. C. (1990). Expression of gap junction channels in communication-incompetent cells after stable transfection with cDNA encoding connexin 32. *Proceedings of the National Academy of Sciences of the USA* **87**, 1328–1331.

Gao, Y. & Spray, D. C. (1998). Structural changes in lenses of mice lacking the gap junction protein connexin43. *Investigative Opthalmology & Visual Science* **39**, 1198–1209.

Gong, X. H., Li, E., Klier, G., Huang, Q., Wu, Y., Lei, H., Kumar, N. M., Horowitz, J. & Gilula, N. B. (1997). Disruption of α_3 connexin gene leads to proteolysis and cataractogenesis in mice. *Cell* **91**, 833–843.

Goodenough, D. A. (1992). The crystalline lens. A system networked by gap junctional intercellular communication. *Seminars in Cell Biology* **3**, 49–58.

Gourdie, R. G., Green, C. R., Severs & Thomson, R. P. (1992). Immunolabeling patterns of gap junction connexins in the developing and mature rat heart. *Anatomy and Embryology* **185**, 363–378.

Harris, A. L., Spray, D. C. & Bennett, M. V. L. (1981). Equilibrium properties of a voltage dependent junctional conductance. *Journal of General Physiology* **77**, 75–94.

Hellmann, P., Winterhager, E. & Spray, D. C. (1996). Properties of connexin40 gap junction channels endogenously expressed and exogenously overexpressed in human choriocarcinoma cell lines. *Pflügers Archiv* **432**, 501–509.

Hille, B. (1992). *Ionic Channels of Excitable Membranes.* pp. 345–357. Sinauer Associates, Inc., Sunderland, MA, USA.

Kistler, J., Kirkland, B. & Bullivant, S. (1985). Identification of a 70,000-D protein in lens membrane junctional domains. *Journal of Cell Biology* **101**, 28–35.

Kwak, B. R., Hermans, M. M., De Jonge, H. R., Lohmann, S. M., Jongsma, H. J. & Chanson, M. (1995). Differential regulation of distinct types of gap junction channels by similar phosphorylating conditions. *Molecular Biology of the Cell* **6**, 1707–1719.

Lin, J. S., Eckert, R., Kistler, J. & Donaldson, P. (1998). Spatial differences in gap junction gating in the lens are a consequence of connexin cleavage. *European Journal of Cell Biology* **76**, 246–250.

Mackay, D., Ionides, A., Berry, V., Moore, A., Bhattacharya, S. & Shiels, A. (1997). A new locus for dominant 'zonular pulverulent' cataract, on chromosome 13. *American Journal of Human Genetics* **60**, 1474–1478.

Manivannan, K., Ramanan, S. V., Mathias, R. T. & Brink, P. R. (1992). Multichannel recordings from membranes which contain gap junctions. *Biophysical Journal* **61**, 216–227.

Mathias, R. T., Rae, J. L. & Baldo, G. J. (1997). Physiological properties of the normal lens. *Physiological Reviews* **77**, 21–50.

Moreno, A. P., Eghbali, B. & Spray, D. C. (1991*a*). Connexin32 gap junction channels in stably transfected cells: unitary conductance. *Biophysical Journal* **60**, 1254–1266.

Moreno, A. P., Eghbali, B. & Spray, D. C. (1991*b*). Connexin32 gap junction channels in stably transfected cells. Equilibrium and kinetic properties. *Biophysical Journal* **60**, 1267–1277.

Moreno, A. P., Fishman, G. I., Beyer, E. C. & Spray, D. C. (1995). Voltage dependent gating and single channel analysis of heterotypic gap junction channels formed of Cx45 and Cx43. In *Intercellular Communication Through Gap Junctions*, ed. Kanno, Y., Kataoka, K., Shiba, Y., Shibata, Y. & Shimazu, T., *Progress in Cell Research*, vol. 4, pp. 405–408. Elsevier, Amsterdam.

Moreno, A. P., Rook, M. B., Fishman, G. I. & Spray, D. C. (1994*a*). Gap junction channels: distinct voltage-sensitive and insensitive conductance states. *Biophysical Journal* **67**, 113–119.

Moreno, A. P., Saez, J. C., Fishman, G. I. & Spray, D. C. (1994*b*). Human connexin43 gap junction channels: Regulation of unitary conductances by phosphorylation. *Circulation Research* **74**, 1050–1057.

Morley, G. E., Ek-Vitorin, J. F., Taffett, S. M. & Delmar, M. (1997). Structure of connexin43 and its regulation by pH_i. *Journal of Cardiovascular Electrophysiology* **8**, 939–951.

Paul, D. L., Ebihara, L., Takemoto, L. J., Swenson, K. I. & Goodenough, D. A. (1991). Connexin46, a novel lens gap junction protein, induces voltage-gated currents in nonjunctional plasma membrane of *Xenopus* oocytes. *Journal of Cell Biology* **115**, 1077–1089.

Ramanan, S. V. & Brink, P. R. (1993). Multichannel recordings from membranes which contain gap junctions II: substates and conductance shifts. *Biophysical Journal* **65**, 1387–1395.

Reed, K. E., Westphale, E. M., Larson, D. M., Wang, H.-Z., Veenstra, R. D. & Beyer, E. C. (1993). Molecular cloning and functional expression of human connexin37, an endothelial cell gap junction protein. *Journal of Clinical Investigation* **91**, 997–1004.

Schutte, M., Chen. S., Buku, A. & Wolosin, J. M. (1998). Connexin50, a gap junction protein of macroglia in the mammalian retina and visual pathway. *Experimental Eye Research* **66**, 605–613.

Shiels, A., Mackay, D., Ionides, A., Berry, V., Moore, A. & Bhattacharya, S. (1998). A missense mutation in the human Connexin50 gene (GJA8) underlies autosomal dominant 'Zonular Pulverulent' cataract, on chromosome 1q. *American Journal of Human Genetics* **62**, 526–532.

Simpson, I., Rose, B. & Loewenstein, W. R. (1977). Size limits of molecules permeating the junctional membrane channels. *Science* **197**, 294–296.

Spray, D. C., Harris, A. L. & Bennett, M. V. L. (1979). Voltage dependence of junctional conductance in early amphibian embryos. *Science* **204**, 432–434.

Steele, E. C. Jr, Lyon, M. F., Glenister, P. H., Guillot, P. & Church, R. L. (1997). Identification of a mutation in the connexin50 (Cx50) gene of the No2 cataractous mouse mutant. In *Gap Junctions*, ed. Werner, R., pp. 289–293. IOS Press, Amsterdam.

Traub, O., Eckert, R., Lichtenberg-Frate, H., Elfgang, C., Bastide, B., Scheidtmann, K. H., Hulser, D. F. & Willecke, K. (1994). Immunochemical and electrophysiological characterisation of murine connexin40 and -43 in mouse tissue and transfected human cells. *European Journal of Cell Biology* **64**, 101–112.

Trexler, E. D., Bennett, M. V. L., Bargiello, T. A. & Verselis, V. K. (1996). Voltage gating and permeation in a gap junction hemichannel. *Proceedings of the National Academy of Sciences of the USA* **93**, 5836–5841.

Veenstra, R. D., Wang, H.-Z., Beblo, D. A., Chilton, M. G., Harris, A. L., Beyer, E. C. & Brink, P. R. (1995). Selectivity of connexin-specific gap junctions does not correlate with channel conductance. *Circulation Research* **77**, 1156–1165.

Veenstra, R. D., Wang, H.-Z., Beyer, E. C. & Brink, P. R. (1994). Selective dye and ionic permeability of gap junction channels formed by connexin45. *Circulation Research* **75**, 483–490.

Verheule, S., van Kempen, M. J. A., et Wlescher, H. J. A., Kwak, B. R. & Jonsgma, H. J. (1997). Characterisation of gap junction channels in adult rabbit atrial and ventricular myocardium. *Circulation Research* **80**, 673–681.

Vogel, R. & Weingart, R. (1998). Mathematical model of vertebrate gap junctions derived from electrical measurements on homotypic and heterotypic channels. *Journal of Physiology* **510**, 177–189.

White, T. W., Bruzzone, R., Goodenough, D. A. & Paul, D. L. (1992). Mouse Cx50, a functional member of the connexin family of gap junction proteins, is the lens fibre protein MP70. *Molecular Biology of the Cell* **3**, 711–720.

White, T. W., Bruzzone, R., Wolfram, S., Paul, D. L. & Goodenough, D. A. (1994). Selective interactions among the multiple connexin proteins expressed in the vertebrate lens: the second extracellular domain is a determinant of compatibility between connexins. *Journal of Cell Biology* **125**, 879–892.

White, T. W., Goodenough, D. A. & Paul, D. L. (1998). Ocular abnormalities in connexin50 knockout mice. *Journal of Cell Biology* **143**, 815–825.

Wilders, R. & Jongsma, H. J. (1992). Limitations of the dual voltage clamp method in assaying conductance and kinetics of gap junction channels. *Biophysical Journal* **63**, 942–953.

Wolosin, J. M., Schutte, M. & Chen, S. (1997). Connexin distribution in the rabbit and rat ciliary body. A case of heterotypic epithelial gap junctions. *Investigative Ophthalmology & Visual Science* **38**, 341–348.

Yancey, S. B., Biswal, S. & Revel, J. P. (1992). Spatial and temporal patterns of distribution of the gap junction protein connexin43 during mouse gastrulation andorganogenesis. *Development* **114**, 203–212.

Yeager, M. & Gilula, N. B. (1992). Membrane topology and quaternary structure of cardiac gap junction ion channels. *Journal of Molecular Biology* **223**, 929–948.

Acknowledgements

This work was supported by NIH grants, NIH-RO1-HL38449 and NIH-RO1-EY08969. The authors would like to thank Ms Marcia Urban and Ms Eileen Craig for their technical assistance.

Corresponding author

D. C. Spray: Department of Neuroscience, 712 Kennedy Centre, Albert Einstein College of Medicine, 1300 Morris Park Avenue, Bronx, NY 10461, USA.

Email: spray@aecom.yu.edu